Study on Prediction Technique of Influence Range from super long-term Natural Phenomenon

Takashi AKIYAMA
The Kansai Electric Power Co. Inc., Japan

***ABSTRACT*:** Civil engineering structures are usually designed to harmonize with the social and natural environments of the chosen construction site.

When it comes to special civil engineering structures that require the maintenance of functionality in the super long-term, it is necessary to choose a geologically stable site due to the significantly uncertain nature of influence from future natural events. Therefore, at first we should predict influence range from natural phenomenon, and it becomes necessary to plan a facility in the geologically-stable area. In the case of civil works structure holding wastes especially such as radioactive wastes, it is necessary to maintain its function for more than 10,000 years. In this case places appropriate for the facility have been limited to an underground which was isolated from the sphere of life. The influence could be calculate that these deep places receive from natural phenomena such as earthquakes, fault activities, volcanic activities, thermal events, ground uplift and erosion, and evaluate the soundness of the facility in the super long- term.

However, there is no established method or standard for assessing the range and probability of such natural events occurring in the super long-term yet. Therefore, it is desirable that the place where it is stable enough geologically and there is little influence from natural phenomenon is to be chosen for the candidate site.

This paper examines the case of fault activities and explores the method for predicting the range of influence from natural events in the super long-term, to be used as a tool for site selection with minimal influence. Using this technique proposing candidate area conservatively beforehand, we can reduce the risk of change of the candidate site for wastes in the field-survey stage.

KEYWORDS : super long-term, prediction technique of influence range, probability density function

1. INTRODUCTION

The range of influence from the branching and extension of known active faults and folds must be assessed appropriately in order to prevent fault activities from directly damaging underground disposal facilities for high-level radioactive waste and actual waste drums stored therein. In the stage of selecting preliminary investigation areas, the Nuclear Waste Management Organization of Japan[1)] stipulates the exclusion of areas that contain documented known faults as well as areas that (1) are within the active fault range (fault fracture zone) as well as the deformation zone around such range, (2) are likely to contain an active fault splay (bifurcation) or (3) contain active folds or flexures that have shown continuation of significant activities. However, the Organization does not present specific numerical indicators concerning affected areas.

Meanwhile, as for the temporal scale of long-term safety assurance to be considered in geological disposal, the Organization says the records from the last several hundred thousand years to several million years should be examined to geo-scientifically verify activities of natural phenomena over the next 100,000 years[1)]. There is a possibility that the safety over the next million

years might have to be assessed so as to assure even a higher level of safety.

The state of tectonic stress that governs the activities of active faults and folds in Japan is believed to maintain a specific tendency in the temporal scale of several hundred thousand years to several million years. Future projection in the order of 100,000 years could produce assessment that anticipates the current continuity of plate tectonics. However, future projection in the order of a million years may be affected by the margin of error in parameters required in such assessment. In other words, it is necessary to quantify the scale of data fluctuations that arise even on the assumption that tectonic activities remain constant.

This study seeks to present specific probabilistic numerical indicators concerning the range of the influence of active faults for the next million years in consideration of activity characteristics such as local properties and types of currently-identified active faults in Japan, even though the basic data used in case analysis is limited, and despite numerous assumptions included in the study approach.

2. EXAMINATION METHOD AND FLOW

The influence of active faults in this study is assessed as the probability at which the faults affect their surrounding area and underground disposal facilities. This is determined through combining secondary probabilities that take into account the extension along the fault direction and branching along the fault sides of known active faults (Fig. 1). The fault length and the amount of branching along the sides of faults, which is a basic parameter, relate to two-dimensional shapes, and the range of influence in the depth direction is not considered.

Fig. 2 shows the flow of examinations in this assessment method.

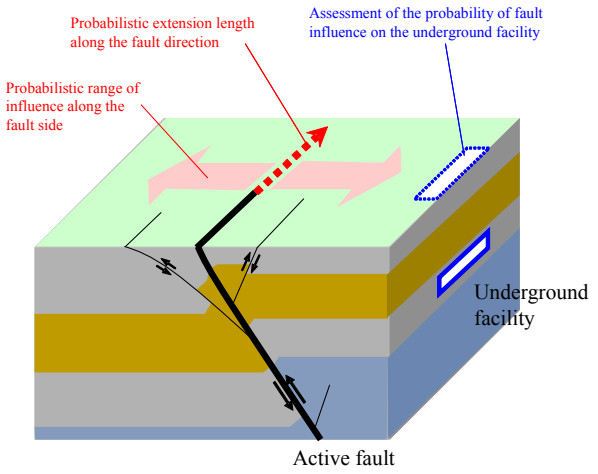

Fig.1 Outline of branching and extension resulting from fault activities, and its probabilistic assessment

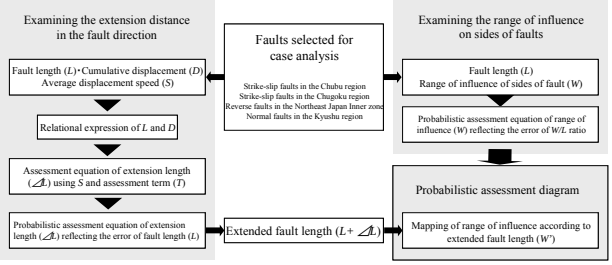

Fig.2 The flow of examining the probabilistic assessment of fault activities

In view of the types of active faults that exist in this country, the case analysis covered typical faults in the strike-slip type, reverse dip-slip type and normal dip-slip type. In regard to the strike-slip type, the analysis used the faults in the Chubu and Chugoku regions with parameters already defined by Matsuda et al.[2]. However, since the document contains systematic parameter differences between faults in the Chubu region and faults in the Chugoku region, they have been handled as faults in separate groups for statistical considerations. As for reverse faults, even though many of them are distributed from the Kinki region eastwards, the analysis has used several faults belonging to the Northeast Japan Inner Zone, as categorized according to seismic geological structures by Kakimi et al.[3], which are active in the east-west compressive stress field and went active approximately around the same period. Since the distribution of normal faults is generally limited to the Kyushu region, the analysis has used several faults from this region.

In examining the distance of fault extension along its direction, this study has considered the correlation between fault length and cumulative displacement, and sorted the individual findings according to the fault type and region to work out a relational expression. The increase of displacement, obtained as the product of average displacement speed and assessment period, is then inserted into the expression to estimate the length of fault extension in the next one million years. In view of the margin of error for fault length in the relational expression, the study has determined a probability density function that reflects the distribution of error and obtained a probabilistic extension length according to the function.

Meanwhile, in examining the range of influence in the lateral direction, the study has measured the distance between a main fault and its branching fault on the active fault distribution map, and determined a probability density function for the ratio of the influence width to fault length so as to obtain a probabilistic influence range in the lateral direction.

The probabilistic assessment diagram, which is the final objective of this study, is a 2D presentation of probabilistic fault lengths in one million years, obtained in the examination of extension distance, as well as their probabilistic range of influence in the lateral direction.

3. ASSESSMENT ON FAULTS' EXTENSION DISTANCE IN THE FAULT DIRECTION

3.1 Assessment approach

Equation (1) is widely used to indicate the relationship between fault length (L) and cumulative displacement (D). [4), 5), 6)]

$$D = cL^n \quad (1)$$

In Equation (1), c and n refer to figures specific to the applicable fault group. "n" represents the order of the function, and can be obtained as a gradient by plotting multiple fault length and displacement figures in a double-logarithmic graph. Equation (1) may be transposed into Linear Equation (2) on a double-logarithmic graph, indicating the fault length as a function of displacement:

$$\log L = 1/n \log D - 1/n \log c \quad (2)$$

In overseas cases, n is equal to or greater than 1. If n=1, the active fault is growing proportionate to the increase of displacement. The greater n is, the growth of the fault becomes tapered with the increase of displacement [4), 5), 6)]. The mechanism of fault growth deceleration is attributed to, for example, the presence of concealed faults that existed prior to the applicable fault activity, or explained with the "alternative growth model" [6)] that consider interactions in the fault tip. When n=1, c refers to the critical shear strain[7)], which is a parameter that reflects the physical property of crust or bedrock that developed the fault. In other words, c and n are parameters that depend on fault types and regional characteristics. When applying this equation to predict the growth of active faults in Japan, it is necessary to use parameters that are set according to fault types and regional characteristics in Japan based on various fault data.

When Equation (1) or Equation (2) is used to project future growth of a fault, the growing cumulative displacement is obtained as the product of currently-known faults' average displacement speed (S) and future term of activities (i.e. assessment term, T). While the relationship between the current fault length and cumulative displacement is represented in Equation (1), the relationship between the future fault length (L') and cumulative displacement (D') is indicated in Equation (3).

$$D' = D + ST = cL'^n \quad (3)$$

Equations (1) and (3) provide the deterministic assessment equation (4) to obtain the extension length ($\triangle L$):

$$\triangle L = L' - L = (L^n + ST/c)^{1/n} - L \quad (4)$$

In actual 2D presentation of a fault's extension length,

half of ⊿L, obtained in Equation (4), is used as single-side extension length, as extension is anticipated from both ends of a fault.

3.2 Identifying activity parameters of faults used in the case analysis

Faults listed in Table 1 have been selected to identify the relationship between fault length and cumulative displacement in Japan.

Of parameters required for consideration, fault length and average displacement speed are recorded in various active fault distribution maps and databases. However, cumulative displacement is not generally known except for that of faults that have extensive research data, and therefore has to be estimated on hypothesis based on physiographic and structural geological knowledge.

Some of the strike-slip faults identified by Matsuda et al.[2] are suspected to have been active in and after the Cretaceous period. The document defines the cumulative displacement of such active faults as "Quaternary displacement (Dq)" and treats it separately from the displacement of Cretaceous geologic units. "Quaternary displacement" represents the size of a relatively large V bend, believed to be a water system from the Late Neogene peneplain formation period. The reference year for displacement itself has the margin of error in the order of several hundred thousand years. Generally, the age-reference for strike-slip faults is less accurate than those for reverse faults and normal faults. Their average displacement speed may have the margin of error in the order of logarithm expressed in "activity". Of the faults identified by Matsuda et al.[2], the Goson Fault Zone includes the fault in the seas off the northern Tango Peninsula according to the assessment conducted by the Headquarters for Earthquake Research Promotion[8]. This study adopts this definition.

The length of reverse faults and normal faults is determined based on the long-term assessment[8] conducted by the Headquarters for Earthquake Research Promotion. Of faults covered in the long-term assessment, some are running parallel to each other with some sections overlapping. In this case, the fault length of the overall fault zone is determined based on the fault distribution diagram[8]. As for average displacement speed, the net values listed in the active fault database[9] compiled by the National Institute of Advanced Industrial Science and Technology have been used.

Even for reverse and normal faults, cases that have the cumulative displacement data available from the time of activity onset are very limited. Some assumption was made to set the time of activity onset and make a tentative estimation of cumulative displacement. For reverse faults, since the time when Northeast Japan turned into an intensive compressive stress field (2.4Ma)[10] coincides with the time of activity onset for the eastern margin of the Yokote Basin Fault Zone and the Senya Fault as estimated in the Balanced Cross-Section Approach[11], this age figure has been multiplied with individual fault's average displacement speed to obtain cumulative displacement. For normal faults, since the onset of Okinawa Trough formation is believed to be 1.0-2.0Ma[12] and since Beppu Bay is believed to have emerged during the Pull-apart Basin formation period since 1.5Ma[13] resulting from right-lateral displacement, which is typically attributed to many normal faults in the Kyushu region, these age figures have been multiplied with individual fault's average displacement speed to obtain cumulative displacement.

Table 1 Faults with examined extension length in the fault direction and parameters

A : Strike-slip faults in the Chubu and Chugoku regions

	Source	Partially reproduced and added to Table No.1 (a), (b) of Matsuda et al. [2]											
	Fault (zone) name	Fault length (Note 1)				Quaternary displacement (Note 2)				Average displacement speed (Note 3)			
		L(km)			log L	Dq(km)			log Dq	S(mm/y)			log S
		Minimum	Maximum	Median		Minimum	Maximum	Median		Minimum	Maximum	Median	
Chubu	Tanna Fault Zone			30.0	1.48			1.00	0.00			2.00	0.30
	Itoigawa-Shizuoka Tectonic Line			145.0	2.16			12.00	1.08	8.0	10.0	9.00	0.95
	Shinanozaka Fault Zone	24.0	25.0	24.5	1.39	0.2	0.3	0.25	-0.60	0.05	1.0	0.53	-0.28
	Ushikubi Fault Zone	54.0	56.0	55.0	1.74	1.0	2.0	1.50	0.18	1.0	5.0	3.00	0.48
	Mozumi Fault Zone			45.0	1.65	0.2	1.0	0.60	-0.22	1.0	2.0	1.50	0.18
	Atotsugawa Fault Zone			61.0	1.79	2.0	3.0	2.50	0.40	2.0	5.0	3.50	0.54
	Takayama Fault Zone			48.0	1.68	1.0	2.5	1.75	0.24			1.00	0.00
	Sakaitoge Fault Zone			50.0	1.70			3.00	0.48	1.0	6.0	3.50	0.54
	Atera Fault Zone	60.0	68.0	64.0	1.81	6.0	7.5	6.75	0.83	3.0	5.0	4.00	0.60
	Onedani Fault Zone			70.0	1.85			2.00	0.30			2.00	0.30
	Mugigawa Fault Zone			28.0	1.45			0.30	-0.52	0.1	0.9	0.50	-0.30
	Upper Nagaragawa Fault Zone			30.0	1.48	0.3	1.1	0.70	-0.15	0.1	0.9	0.50	-0.30
	Ibigawa Fault Zone			25.0	1.40			1.00	0.00	0.1	0.9	0.50	-0.30
	Okukonami Fault Zone			12.0	1.08	0.1	0.2	0.15	-0.82	0.05	0.5	0.28	-0.56
Chugoku	Kanbayashigawa Fault Zone	18.0	27.0	22.5	1.35			0.08	-1.10	0.1	0.2	0.15	-0.82
	Goson Fault Zone (Note 3)			34.0	1.53			0.10	-1.00	0.05	0.5	0.28	-0.56
	Yamada Fault Zone	27.0	33.0	30.0	1.48			0.40	-0.40	0.05	0.5	0.28	-0.56
	Mitoke-Kameoka Fault Zone	52.0	60.0	56.0	1.75			0.50	-0.30	0.3	0.5	0.40	-0.40
	Habu Fault Zone	15.0	18.0	16.5	1.22	0.15	0.17	0.16	-0.80	0.2	0.6	0.40	-0.40
	Amadaki-Kamado Fault Zone	11.0	15.0	13.0	1.11			0.10	-1.00	0.05	0.5	0.28	-0.56
	Shikano Fault Zone			15.0	1.18			0.13	-0.89	0.1	0.4	0.25	-0.60
	Yamasaki Fault Zone	80.0	85.0	82.5	1.92	0.3	0.5	0.40	-0.40	0.3	1.0	0.65	-0.19
	Median Tectonic Line (Shikoku)			192.0	2.28	4.0	6.0	5.00	0.70	5.0	10.0	7.50	0.88
	Shinji Fault Zone	18.0	27.0	22.5	1.35	0.15	0.24	0.20	-0.71	0.05	0.5	0.28	-0.56
	Iwakuni Fault Zone	40.0	47.0	43.5	1.64	0.2	2.5	1.35	0.13	0.1	1.0	0.55	-0.26
	Kikugawa Fault Zone			32.0	1.51	0.5	0.58	0.54	-0.27	0.1	0.9	0.50	-0.30

Note 1 The linear distance connecting fault ends (according to source)
Note 2 The size of a relatively large V bend, believed to be a water system from mainly the peneplain formation period (Late Neogene) (according to source)
Note 3 The fault length of the Goson Fault Zone includes the fault in the seas off the northern Tango Peninsula according to the assessment of the Headquarters for Earthquake Research Promotion
Note 4 In cases when each parameter was shown as a range, the median was used

B : Reverse faults in the Northeast Japan Inner Zone

Source	Headquarters for Earthquake Research Promotion [8]		Active fault database of the National Institute of Advanced Industrial Science and Technology [9]			
Fault (zone) name	Fault length		Net values of average displacement speed		Cumulative displacement (Note 5)	
	L(km)	log L	S(mm/y)	log S	D(km)	log D
Kuromatsu Inner Lowland Fault Zone	32.0	1.51	1.00	0.00	2.40	0.38
Western Marginal Fault Zone of the Hakodate Plain	24.0	1.38	0.40	-0.40	0.96	-0.02
Western Marginal Fault of the Tsugaru Mountains	16.0	1.20	0.30	-0.52	0.72	-0.14
Kuroishi Fault	23.0	1.36	0.20	-0.70	0.48	-0.32
Fault of the West Coast of Aomori Bay	31.0	1.49	0.80	-0.10	1.92	0.28
Eastern Marginal Fault Zone of the Yokote Basin	56.0	1.75	0.80	-0.10	1.92	0.28

Note 5 The cumulative displacement is obtained by multiplying the average displacement speed with the number of years (2.4Ma) after Northeast Japan turned into an intensive compressive stress field

C : Normal faults in Kyushu region

Source	Headquarters for Earthquake Research Promotion [8]		Active fault database of the National Institute of Advanced Industrial Science and Technology [9]			
Fault (zone) name	Fault length (Note 6)		Net values of average displacement speed		Cumulative displacement (Note 7)	
	L(km)	log L	S(mm/y)	log S	D(km)	log D
Beppu-Haneyama Fault Zone	92.0	1.96	3.10	0.49	4.65	0.67
Unzen Fault Group	59.0	1.77	3.00	0.48	4.50	0.65
Futagawa-Hinagu Fault Zone	101.0	2.00	0.90	-0.05	1.35	0.13
Izumi Fault Zone	20.0	1.30	0.30	-0.52	0.45	-0.35
Mino Fault Zone	24.0	1.38	0.20	-0.70	0.30	-0.52

Note 6 In cases when fault lengths overlap in areas where some faults run parallel, it is measured based on the fault distribution diagram of the source
Note 7 The cumulative displacement is obtained by multiplying the average displacement speed with the number of years (1.5Ma) after the start of the Pull-apart formation of Beppu Bay

3.3 Deterministic assessment of extension distance

Figure 3 shows plots in a double-logarithmic graph of selected fault length and cumulative displacement figures, as well as the mapping's approximation equation. The approximation equations for each fault type and regional group are as follows:

Strike-slip faults in the Chubu region: $\log L = \log 0.442D + 1.580$ $(D = 0.000267L^{2.26})$ (5)

Strike-slip faults in the Chugoku region: $\log L = \log 0.526D + 1.790$ $(D = 0.000395L^{1.90})$ (6)

Reverse faults in the Northeast Japan Inner Zone: $\log L = \log 0.467D + 1.412$ $(D = 0.000940L^{2.14})$ (7)

Normal faults in the Kyushu region: $\log L = \log 0.475D + 1.629$ $(D = 0.000370L^{2.11})$ (8)

The coefficient of correlation for each of the plots by fault type and region was the greatest at 0.90 for strike-slip faults in the Chubu region, and the smallest at 0.71 for reverse faults in the Northeast Japan Inner Zone, indicating a relatively good correlation as parameters for active faults. Matsuda et al.[2] have pointed to independent mapping trends between strike-slip faults in the Chubu and Chugoku regions despite the use of the same approach in identifying fault length and cumulative displacement, suggesting regional variations in fault extension characteristics.

3.4 Probabilistic assessment of extension distance and probability definition

Fig.3 shows that the plots for each of the fault types and regions have dispersion against the respective approximate curves.

Such dispersion is attributed to deviation of individual faults from average activity for the applicable fault type and region (individual faults' deviation) and deviation arising from the estimation of average displacement speed used to obtain cumulative displacement (technical deviation due to measurement accuracy).

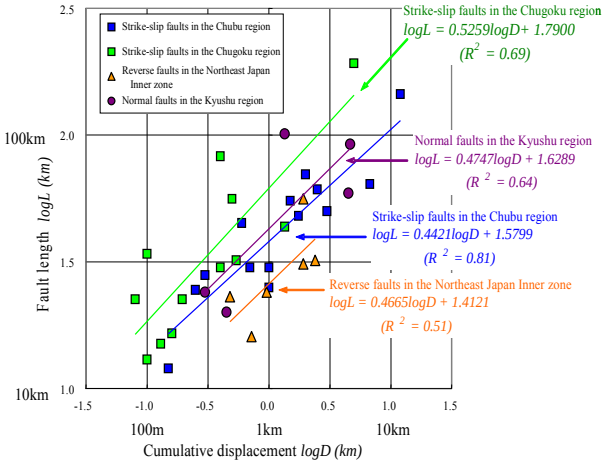

Fig.3 The relationship between fault length and cumulative displacement according to fault type and region, and its approximation equation

The probability density function indicated by the distribution of fault length error (distribution of error for the fault length ratio on the logarithmic axis) against approximate curves differs for individual fault-types and regions. However, with the limited number of data sets in this study, it is difficult to make statistical considerations, as shown in several plots for reverse faults in the Northeast Japan Inner Zone and normal faults in the Kyushu region. Compiling the deviation of all plots from their respective approximate curves into a histogram points to log-normal distribution described with a probability density function, although it is slightly asymmetrical (Fig.4). It is therefore assumed that the deviation of individual faults from approximate curves according to fault type and region observes log-normal distribution with the standard deviation of data from the respective approximate curves as parameters.

The standard deviation (σ) of plots for various fault types and regions against approximation is as follows:

Strike-slip faults in the Chubu: $\sigma=0.115$ (9)

Strike-slip faults in the Chugoku: $\sigma=0.187$ (10)

Reverse faults in the Northeast Japan Inner Zone: $\sigma=0.128$ (11)

Normal faults in the Kyushu: $\sigma = 0.196$ (12)

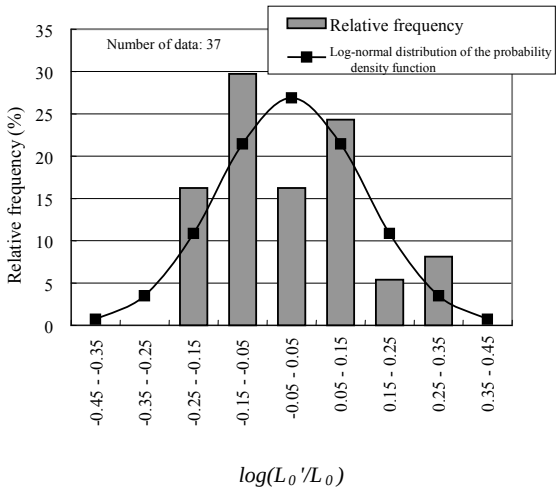

Fig.4 Distribution of fault length error against approximate curves and supposed log-normal distribution of the probability density function
Lo'/Lo is the ratio of fault length from current cumulative displacement to fault length on the approximate line

Incidentally, the deviation from approximate curves shown in Fig.4 and equations (9) – (12) represents deviation of fault length in all cases, rather than deviation of extension length. When obtaining extension length from approximate straight line with deviation (Nσ) in a double-logarithmic graph indicating the relationship between fault length and cumulative displacement, the effect of the deviation on fault extension length is as follows:

The current fault length (L_0) and fault length in one million years (L_{100}) on the approximate straight line, and the current fault length (L'_0) and fault length in one million years ((L'_{100}) on the straight line indicating deviation (Nσ) and running parallel to the approximate straight line, have the following relationship:

$$L'_0 / L_0 = L'_{100} / L_{100} = 10^{N\sigma} \quad (13)$$

Since the deviation of extension length is indicated as the difference between the extension length ($\triangle L'$) with deviation (Nσ) and extension length ($\triangle L$) according to approximation, the equation (14) is obtained:

$$\triangle L' - \triangle L = (L'_{100} - L'_0)) - (L_{100} - L_0)$$

Due to equation (13): $= 10^{N\sigma}(L_{100} - L_0) - (L_{100} - L_0)$

$$= (10^{N\sigma} - 1)\ \triangle L \quad (14)$$

Fig.5 shows the deviation between the single-side extension length obtained by inserting n and c based on equations (5) – (8) into equation (4), and the deviation of single-side extension length obtained by inserting the standard deviation (σ) based on equations (9) – (12) into equation (14), calculated for all of the faults subject to this study.

In this study's estimation, due to the difference in approximation coefficient in (5) – (8), the extension length for strike-slip faults in the Chugoku region is assessed to be large, while the extension length for reverse faults in the Northeast Japan Inner Zone is assessed to be small. Among faults of the same type and region, extension length tends to be large for faults that currently have a short fault length and high average displacement speed. The margin of extension length is in accordance with log-normal distribution. With the deviation of +2σ, the error of extension length is approximately twice the deterministic extension length.

4. ASSESSMENT ON THE RANGE OF INFLUENCE IN THE LATERAL DIRECTION

4.1 Assessment approach

(1) Relationship between the influence width and fault length in the lateral direction

The width of the deformation zone containing fracture zones, process zones, etc. that forms along the sides of faults as a result of fault activities is known to be generally proportionate to the length of the applicable fault.

Ogata[14] indicated an empirical equation on fault width (width of a fault area including multiple fractures; FW) and fault length (L) based on a foundation bedrock survey conducted for electric power facilities. The equation can be described as exponential function as follows[15]:

$$FW = 1.65 \times 10^{-3} L^{1.15} \quad (15)$$

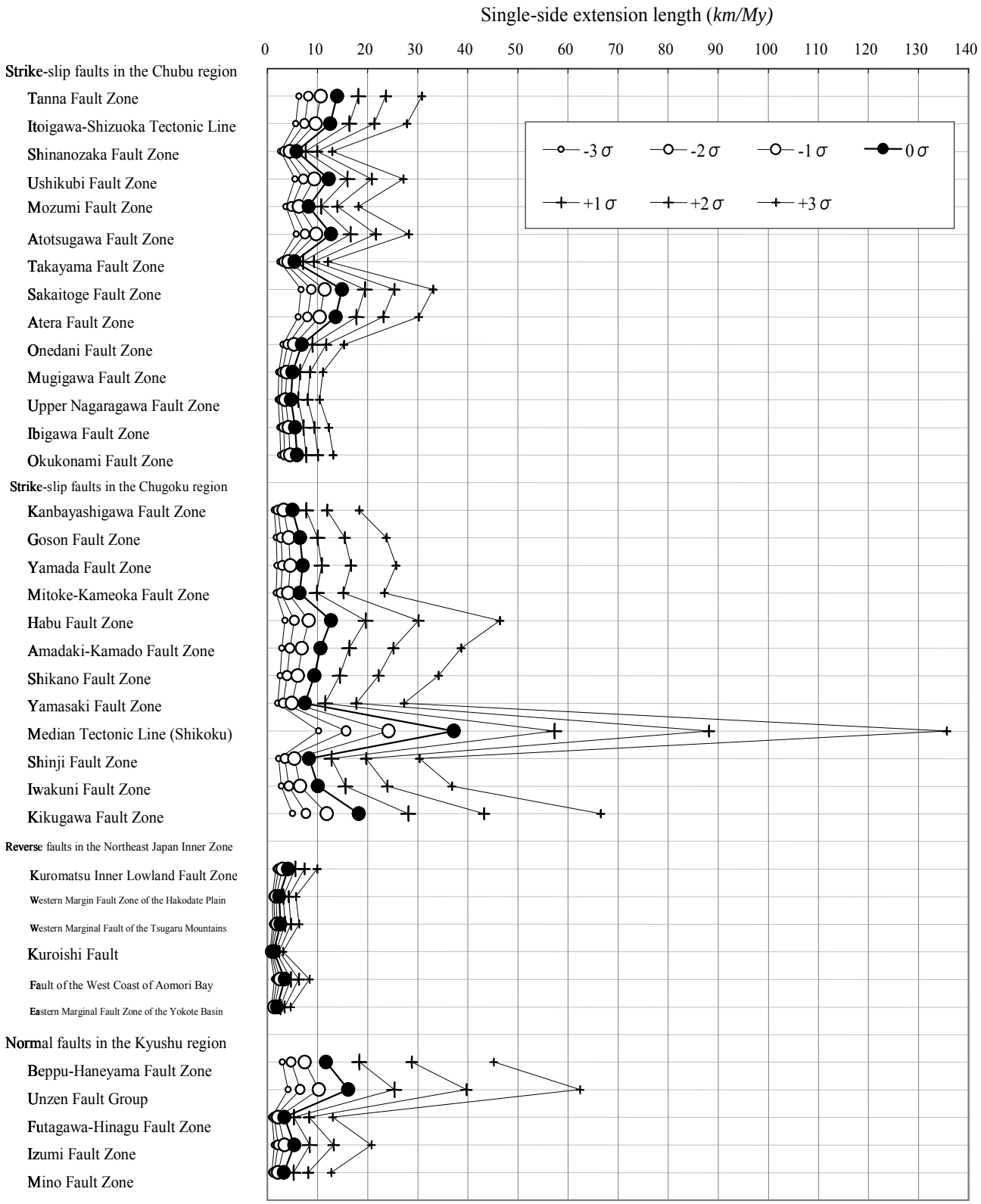

Fig.5 The single-side extension length of the selected 37 faults over the next million years and its deviation

The width of process zone (PW)[16], formed alongside a fault (containing an area that consists of fault rocks of the fracture zone, cataclasite zone, etc. and an area damaged with joints and secondary shear cracks at a density higher than that seen in the surrounding host rocks), and fault length (L) are also known to have the relationship shown below. Japan's three faults (Atotsugawa Fault[15], Usukidani Fault[15] and Adera Fault[17]) show consistent tendency. The width of process zone is approx. 10 times the fault width indicated by Ogata[14].

$$PW = 1.6\times10\text{-}2\ L \qquad (16)$$

Such an empirical equation does not describe the relationship between an active fault and its surrounding fault splays, but represents fault's basic geometric characteristic. In estimating the range of lateral fault influence due to branching, the ratio of the width of the range of influence to the fault length (W/L) can be used to achieve quantifiable assessment.

(2) Considerations according to fault types

The abovementioned relationship between fault width, process zone width and fault length is typically based on studies on strike-slip faults. Well-known examples of lateral branching in strike-slip faults include stepovers, associated flower structures and splay structures at fault ends[18]. Such structures are commonly seen in strike-slip faults in Japan as well. In the case of reverse faults in Japan, many cases of frontal shift in the subsidence side and back thrust in the uplift side have been reported [19]. In the case of normal faults, broad half and full grabens are formed on the subsidence side, creating occasional synthetic / antithetic faults inside [20].

These differences in branching fault format arise from the variation of stress distribution around faults according to fault types. Fault types should therefore affect the range of influence in the same way. In the case of reverse and normal faults, the mechanism of fault branching is different on the uplift and subsidence sides, making it also necessary to perform separate assessment for the uplift and subsidence sides.

4.2 Faults covered in case analysis and method for measuring the range of influence

In order to determine the range of fault's influence in the lateral direction, the maximum distance between a main fault and its splay faults is measured for each of the fault types and regions.

Fig.6 shows the concept of the measurement method and its description for each fault type.

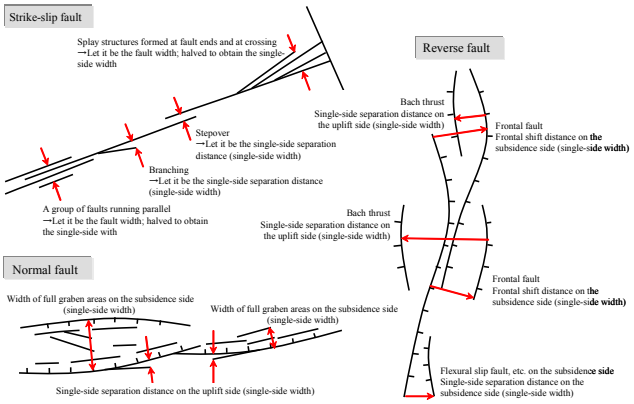

Fig.6 Concept of the measurement method for the maximum separation distance

(1)Strike-slip faults

Of strike-slip faults in the Chubu and Chugoku regions selected by Matsuda et al. 2), those that have the active fault distribution maps published in the long-term assessment by the Headquarters for Earthquake Research Promotion [8] are covered.

Strike-slip faults may branch in more common lateral splay or in the stepover structure. The stepover separation distance is defined as the single-side separation distance. In the case of a group of faults running parallel to each other with no clear main fault, the overall width of all the faults is halved to obtain the single-side separation distance. At an end of a fault or at the crossing with another conjugate fault, a "splay" spreading branching structure may sometimes emerge. In these cases, the overall width is also halved to obtain the

single-side separation distance, but their data has been aggregated separately due to the presence of special stress conditions.

(2)Reverse fault

Reverse faults in the Northeast Japan Inner Zone, used in the case analysis of extension distance, are covered. The active fault distribution maps used in the measurement are those from long-term assessment by the Headquarters for Earthquake Research Promotion[8], but those published by Ikeda et al.[19] are also used in some cases.

Reverse faults often form a raised arc shape toward the subsidence side, with multiple arcuate faults running parallel to each other. In a group of parallel faults, those on the uplift side are generally called "piedmont fault", while those on the subsidence side are called "frontal fault". "Frontal fault" is typically seen as a newer fault formed as a result of frontal shift in "piedmont fault". The separation distance for "frontal fault" and "piedmont fault" is determined as the single-side separation distance on the subsidence side. The uplift side of reverse faults often has secondary faults that show displacement sense in the reverse of that of the main fault, known as back thrust. The separation distance between the main fault and back thrust is determined as the single-side separation distance on the uplift side.

(3)Normal faults

Normal faults in the Kyushu region, used in the case analysis of extension distance, are covered. The active fault distribution maps used in the measurement are those from long-term assessment by the Headquarters for Earthquake Research Promotion 8).

Normal faults often form broad full or half grabens, containing numerous secondary faults inside. There are cases in which the location of the main fault cannot be identified due to the distribution of numerous short faults. Including these cases, the width of full or half graben areas consisting of faults is determined as the single-side separation distance on the subsidence side. When the main fault is identified with secondary faults branching or running in parallel on the uplift side, the single-side separation distance on the uplift side has been measured.

4.3 Examination of the results of influence range measurements

Fig.7 shows the ratio of maximum single-side separation distance to fault length (Wmax/L ratio) based on the measurement, sorted by fault type and region. Strike-slip faults are sorted by region with separate data compiled for splay structures formed at fault ends and at crossings with other faults. For reverse and normal faults, data for the uplift side and the subsidence side are separately shown. The figure indicates the following trends:

1) There is no difference in Wmax/L ratio between strike-slip faults in the Chubu region and those in the Chugoku region. The highest ratio for splay structures that form at fault ends and at crossing with other faults is at about the same level as that for other branching structures. Accordingly, the faults in the Chubu and Chugoku regions are to be treated the same when assessing the range of influence from strike-slip faults. Similarly, no special considerations are given to fault ends, etc.

2) The Wmax/L ratio for reverse faults is greater than that of strike-slip faults both on the uplift and subsidence sides. The average Wmax/L ratio on the uplift and subsidence sides is approximately the same, but the uplift side has a higher top ratio.

3) As for normal faults, the Wmax/L ratio on the subsidence side is three times larger than that on the uplift side.

Based on the abovementioned observations, probabilistic examination on the range of influence in the lateral direction covers strike-slip faults,

	Fault length (km)	Measured location	Characteristic of width	Maximum single-side separation distance (km)	Maximum single-side separation distance to fault length ratio
Strike-slip faults in the Chubu region (common section)					
Upper Nagaragawa Fault Zone	30.0	Between Hachiman Fault and Naru Fault Zone	Fault zone width	2.75	0.092
Tanna Fault Zone	30.0	Between Asahidaki Fault and Upper Toshikawa Fault	Single-side separation distance	2.50	0.083
Ushikubi Fault Zone	55.0	Between Ushikubi Fault and Mannamitoge Fault	Single-side separation distance	4.00	0.073
Tanna Fault Zone	30.0	Between Tanna Fault and the branching fault on the west side	Single-side separation distance	2.00	0.067
Upper Nagaragawa Fault Zone	30.0	Hachiman Fault/Futsukamachi Fault	Stepover distance	2.00	0.067
Ushikubi Fault Zone	55.0	Between Ushikubi Fault and the fault running parallel on the east side	Single-side separation distance	3.50	0.064
Tanna Fault Zone	30.0	Tsuchisawa Fault branching section	Fault zone width	1.75	0.058
Tanna Fault Zone	30.0	Between Tannna Fault and the fault running parallel on the east side	Single-side separation distance	1.50	0.050
Takayama Fault Zone	48.0	Between Genjitake Fault and Miyatoge Fault	Fault zone width	2.25	0.047
Takayama Fault Zone	48.0	Between Enako Fault and Miyatoge Fault	Fault zone width	2.00	0.042
Takayama Fault Zone	48.0	Between Oppara Fault and the branching fault on the west side	Fault zone width	2.00	0.042
Atotsugawa Fault Zone	61.0	Between Atotsugawa Fault and Mozumi-Sukenobu Fault	Fault zone width	2.25	0.037
Atotsugawa Fault Zone	61.0	Between Atotsugawa Fault and Tengudaira Fault	Fault zone width	2.00	0.033
Atotsugawa Fault Zone	61.0	Between Atotsugawa branching fault and Mozumi-Sukenobu Fault	Fault zone width	2.00	0.033
Sakaitoge Fault Zone	50.0	Between Sakaitoge Fault and the fault running parallel on the west side	Single-side separation distance	1.50	0.030
Sakaitoge Fault Zone	50.0	Between Sakaitoge Fault and Kamiya Fault	Stepover distance	1.50	0.030
Atotsugawa Fault Zone	61.0	Between Atotsugawa Fault and fault running parallel on the north side	Single-side separation distance	1.50	0.025
Atera Fault Zone	64.0	Between Atera Fault and the fault running parallel on the east side (Owada)	Single-side separation distance	1.50	0.023
Takayama Fault Zone	48.0	Between Oppara Fault and the southern branching fault	Single-side separation distance	1.00	0.021
Atera Fault Zone	64.0	Between Atera Fault and the fault running parallel on the west side	Single-side separation distance	0.50	0.008
Strike-slip faults in the Chubu region (fault ends and crossings)					
Onedani Fault Zone (Mugigawa/Ibigawa)	70.0	Between northwest end of Nukumi Fault and Ibigawa Fault	Fault width at enlarged fault ends	5.25	0.075
Onedani Fault Zone (Mugigawa/Ibigawa)	70.0	Between central crossing of Nukumi Fault and Ibigawa Fault	Fault width at enlarged fault crossings	5.00	0.071
Atera Fault Zone	64.0	Between Hagiwara Fault and northwest end of branching fault (Oyama)	Fault width at enlarged fault ends	4.50	0.070
Onedani Fault Zone (Mugigawa/Ibigawa)	70.0	Between southeast end branching of Mitahora Fault and Mugigawa Fault	Fault width at enlarged fault ends	4.25	0.061
Atera Fault Zone	64.0	Between Yugamine Fault and northwest end branching fault (Miyachi)	Fault width at enlarged fault ends	3.50	0.055
Atera Fault Zone	64.0	Between Atera Fault and southeast end branching fault (Jogayama)	Fault width at enlarged fault ends	1.75	0.027
Strike-slip faults in the Chugoku region (common section)					
Goson Fault Zone	34.0	Faults in the seas off the northern Tango Peninsula	Fault zone width	2.50	0.074
Iwakuni Fault Zone	43.5	Between Otake Fault and Iwakuni Fault	Single-side separation distance	3.00	0.069
Goson Fault Zone	34.0	Between Goson Fault and the fault running parallel eastward	Fault zone width	2.00	0.059
Mitoke-Kameoka Fault Zone	56.0	Between Mitoke Fault and Kyoto Nishiyama Fault	Fault zone width (stepover)	3.25	0.058
Iwakuni Fault Zone	43.5	Between Otake Fault and Obata Fault	Single-side separation distance	2.50	0.057
Yamada Fault Zone	30.0	Between the fault west of Mt. Miroku and the fault running parallel	Single-side separation distance	1.50	0.050
Mitoke-Kameoka Fault Zone	56.0	Between Kamiyoshi Fault and Kameoka Fault	Fault zone width	2.50	0.045
Mitoke-Kameoka Fault Zone	56.0	Between Koshihata Fault and Kameoka Fault	Fault zone width	2.50	0.045
Kikugawa Fault Zone	32.0	Between Kikugawa Fault and the fault off Kanda-misaki	Stepover distance	1.00	0.031
Mitoke-Kameoka Fault Zone	56.0	Between Koshihata Fault and northward branching fault	Single-side separation distance	1.50	0.027
Yamasaki Fault Zone	82.5	Between Oppara Fault and Hijima Fault	Stepover distance	2.00	0.024
Kanbayashigawa Fault Zone	22.5	Southwestern Kanbayashigawa Fault	Stepover distance	0.50	0.022
Mitoke-Kameoka Fault Zone	56.0	Between Kameoka Fault and westward branching fault	Single-side separation distance	1.00	0.018
Kikugawa Fault Zone	32.0	Fault off Kanda-misaki	Stepover distance	0.50	0.016
Strike-slip faults in the Chugoku region (fault ends and crossings)					
Yamada Fault Zone	30.0	Between Yamada Fault and northward branching fault	Fault width at enlarged fault crossings	2.00	0.067
Yamasaki Fault Zone	82.5	Between branching faults at the eastern end	Fault width at enlarged fault ends	4.75	0.058
Iwakuni Fault Zone	43.5	Between Okawachi Fault and branched ended Kumage Fault	Fault width at enlarged fault ends	2.25	0.052
Kikugawa Fault Zone	32.0	Between Kikugawa Fault and brached ended fault	Fault width at enlarged fault ends	1.50	0.047
Reverse faults in Northeast Japan Inner Zone (uplift side)					
Western Marginal Fault Zone of the Tsugaru Mountains	16.0	Between northern Western Marginal Fault of the Tsugaru Mountains and Namioka Flexure	Single-side separation distance on the uplift side	4.50	0.281
Western Marginal Fault Zone of the Tsugaru Mountains	16.0	Between northern Western Marginal Fault of the Tsugaru Mountains and Yamakoshi Fault	Single-side separation distance on the uplift side	3.00	0.188
Western Margin Fault Zone of the Hakodate Plain	24.0	Between northern Oshima-ohno Fault and back thrust	Single-side separation distance on the uplift side	2.50	0.104
Western Marginal Fault Zone of the Tsugaru Mountains	16.0	Between northern Western Marginal Fault of the Tsugaru Mountains and Iizume Fault	Single-side separation distance on the uplift side	1.50	0.094
Kuroishi Fault	23.0	Between southern Kuroishi Fault and back thrust	Single-side separation distance on the uplift side	2.00	0.087
Western Margin Fault Zone of the Hakodate Plain	24.0	Between southern end of Oshima-ohno Fault (waters) and back thrust	Single-side separation distance on the uplift side	1.50	0.063
Western Marginal Fault Zone of the Tsugaru Mountains	16.0	Between northern Western Marginal Fault of the Tsugaru Mountains and Otai Fault	Single-side separation distance on the uplift side	1.00	0.063
Western Marginal Fault Zone of the Tsugaru Mountains	16.0	Between Namioka Flexure and back thrust	Single-side separation distance on the uplift side	1.00	0.063
Eastern Marginal Fault Zone of the Yokote Basin	56.0	Between Senya Fault and back thrust	Single-side separation distance on the uplift side	3.00	0.054
Kuromatsu Inner Lowland Fault Zone	32.0	Between blind flexure fault and Chiraigawa-ugan Fault	Single-side separation distance on the uplift side	1.50	0.047
Hakodate Plain Western Margin Fault Zone	24.0	Between northern end of Oshima-ohno Fault and back thrust	Single-side separation distance on the uplift side	1.00	0.042
Hakodate Plain Western Margin Fault Zone	24.0	Between southern end of Oshima-ohno Fault and back thrust	Single-side separation distance on the uplift side	1.00	0.042
Kuromatsu Inner Lowland Fault Zone	32.0	Between blind flexure fault and Asahino Fault	Single-side separation distance on the uplift side	1.00	0.031
Kuromatsu Inner Lowland Fault Zone	32.0	Between blind flexure fault and Imunosugawa Fault	Single-side separation distance on the uplift side	1.00	0.031
Eastern Marginal Fault Zone of the Yokote Basin	56.0	Between northern Shiraiwa-Rokugo Fault Group and back thrust	Single-side separation distance on the uplift side	1.50	0.027
Eastern Marginal Fault Zone of the Yokote Basin	56.0	Between Sugisawa Fault and back thrust	Single-side separation distance on the uplift side	1.50	0.027
Kuroishi Fault	23.0	Between northern Kuroishi Fault and back thrust	Single-side separation distance on the uplift side	0.50	0.022
Reverse faults in Northeast Japan Inner Zone (subsidence side)					
Kuromatsu Inner Lowland Fault Zone	32.0	Between blind flexure fault and the fault near Neppugenya	Single-side separation distance on the subsidence side	5.00	0.156
Fault Zone of the West Coast of Aomori Bay	31.0	Between west Aomori Bay Fault and Nogiwa Fault	Frontal shift distance on the subsidence side	3.50	0.113
Kuromatsu Inner Lowland Fault Zone	32.0	Between blind flexure fault and Neppu Fault	Single-side separation distance on the subsidence side	3.50	0.109
Hakodate Plain Western Margin Fault Zone	24.0	Between central Oshima-ohno Fault and Tomikawa Fault	Frontal shift distance on the subsidence side	2.50	0.104
Hakodate Plain Western Margin Fault Zone	24.0	Between south-central Oshima-ohno Fault and Tomikawa Fault	Frontal shift distance on the subsidence side	2.50	0.104
Kuromatsu Inner Lowland Fault Zone	32.0	Between blind flexure fault and Warabitai Fault	Single-side separation distance on the subsidence side	2.00	0.063
Hakodate Plain Western Margin Fault Zone	24.0	Between southern end of Oshima-ohno Fault and Tomikawa Fault	Frontal shift distance on the subsidence side	1.50	0.063
Eastern Marginal Fault Zone of the Yokote Basin	56.0	Between Senya Fault and frontal fault	Frontal shift distance on the subsidence side	2.50	0.045
Kuroishi Fault	23.0	Between Kuroishi Fault and frontal fault	Frontal shift distance on the subsidence side	1.00	0.043
Kuromatsu Inner Lowland Fault Zone	32.0	Between Oshamambe Fault and the reverse fault running parallel	Single-side separation distance on the subsidence side	1.00	0.031
Eastern Marginal Fault Zone of the Yokote Basin	56.0	Between central Shiraiwa-Rokugo Fault Group and frontal fault	Frontal shift distance on the subsidence side	1.50	0.027
Eastern Marginal Fault Zone of the Yokote Basin	56.0	Between Sugisawa Fault and frontal fault	Frontal shift distance on the subsidence side	0.50	0.009
Normal faults in the Kyushu region (uplift side)					
Futagawa-Hinagu Fault Zone	101.0	Between Shirahata Faulta and Fujino-Deharu Fault	Single-side separation distance on the uplift side	5.5	0.054
Izumi Fault Zone	20.0	Between Uchikoba Fault and Kurigeno Fault	Single-side separation distance on the uplift side	1.0	0.050
Beppu-Haneyama Fault Zone	92.0	Between eastern Beppu Bay-Hijiu Fault and Saganoseki Fault	Single-side separation distance on the uplift side	4.5	0.049
Beppu-Haneyama Fault Zone	92.0	Between central Beppu Bay-Hijiu Fault and the subsidiary fault	Single-side separation distance on the uplift side	4.5	0.049
Futagawa-Hinagu Fault Zone	101.0	Between Hinagu Fault and Koura-Imaizumi Fault	Single-side separation distance on the uplift side	4.5	0.045
Futagawa-Hinagu Fault Zone	101.0	Between Hinagu Fault and Hatato-Sotohira Fault	Single-side separation distance on the uplift side	1.0	0.010
Normal faults in the Kyushu region (subsidence side)					
Unzen Fault Group	59.0	Eastern Unzen Fault Group	Width of full graben areas on the subsidence side	12.5	0.212
Unzen Fault Group	59.0	Western Unzen Fault Group	Width of full graben areas on the subsidence side	12.0	0.203
Beppu-Haneyama Fault Zone	92.0	Central Beppu Bay-Hijiu Fault Zone	Width of full graben areas on the subsidence side	15.5	0.168
Beppu-Haneyama Fault Zone	92.0	Eastern Beppu Bay-Hijiu Fault Zone	Width of full graben areas on the subsidence side	12.0	0.130
Unzen Fault Group	59.0	Western end of Unzen Fault Group	Width of full graben areas on the subsidence side	7.5	0.127
Beppu-Haneyama Fault Zone	92.0	Western Beppu Bay-Hijiu Fault Zone	Width of full graben areas on the subsidence side	11.0	0.120
Beppu-Haneyama Fault Zone	92.0	Eastern Noinedake-Haneyama Fault Zone	Width of full graben areas on the subsidence side	9.5	0.103
Beppu-Haneyama Fault Zone	92.0	Western Noinedake-Haneyama Fault Zone	Width of full graben areas on the subsidence side	8.5	0.092
Mino Fault Zone	24.0	Between Fukumasu Fault and Masuoda Fault	Width of full graben areas on the subsidence side	1.5	0.063
Futagawa-Hinagu Fault Zone	101.0	Yatsushiro Sea Seafloor Fault Group	Width of full graben areas on the subsidence side	3.5	0.035
Mino Fault Zone	24.0	Between Miyazono Fault and Ojwake Fault	Width of full graben areas on the subsidence side	0.5	0.021

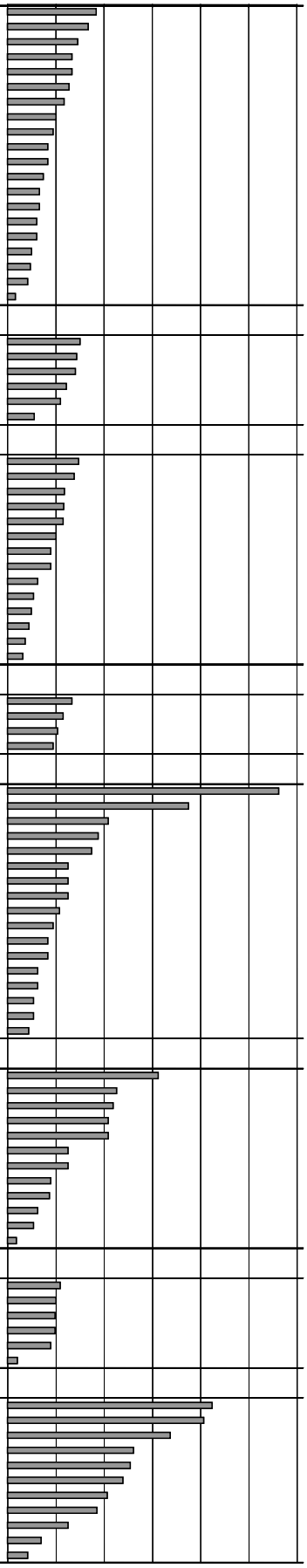

Fig. 7 Comparison of branching fault measurement data and maximum single-side separation distance to fault length ratio

reverse faults (uplift side), reverse faults (subsidence side), normal faults (uplift side) and normal faults (subsidence side).

4.4 Probabilistic assessment of influence range and probability definition

The distribution density of fault cracks in the lateral direction is known to indicate exponential functional distribution against the distance from faults. Vermilye and Scholz[16] showed that the density of microscopic cracks distributed around a fault, decreases at several dozen meters from the fault, and presented an approximate exponential function. The density measurement data of basset-scale cracks in fault process zones in Japan, as shown in Fig.9 (Usukidani Fault) by Kaneori[15] and Fig.4 and Fig.6 (Adera Fault) by Yoshida et al.[17], demonstrates a tendency of exponential functional decline as the distance from the applicable fault increases in the order of 200 to 1,200 meters.

If the distribution density of secondary active faults branching from an active fault can be measured accurately from a statistical perspective, e.g. setting up courses of traverse at a set interval, it is possible to obtain exponential distribution as a probabilistic density function that approximates distribution density, thereby enabling the assessment of the "probability of fault activities damaging an underground facility with a specific area".

Incidentally, this study adopted a simplified measurement approach to avoid excessive work volume, merely measuring the maximum separation distance between a main fault and its branching fault on a fault distribution map without measuring fault density. The probability obtained in this study therefore falls short of indicating the "probability of damage". The study approximates the "probability at which, if a fault branches in the future, a specific location becomes within the range of its influence", while ignoring the "probability of such branching occurring". Probability figures would become lower if the "probability of branching" is taken into account.

In this study, the maximum separation distance is measured between a main fault and its branching fault. From the point of branching to the point from which the maximum separation distance is measured, the separation distance between the main fault and its branch fault fluctuates continuously. If it is assumed that the branching angle from the main fault is constant and that the fault is in straight line, substantial measurement data should be obtained on the courses of traverse that run perpendicular to the main fault at a set interval, according to the distance of separation. Based on this notion, the measurement data for maximum separation distance is converted into data for individual courses of traverse to obtain multiple W (separation distance)/L ratios from a single Wmax (maximum separation distance)/L ratio.

Since there are 44 sets of measurement data for strike-slip faults as opposed to up to 17 sets for reverse and normal faults on the uplift and subsidence sides before correction, the correction relative frequency for strike-slip faults has been used to suppose a probability density function (Fig.8). The correction relative frequency for the W/L ratio in strike-slip faults shows high approximation to the single-side probability density function in normal distribution, compared to the probability density function in exponential distribution. Based on the aforementioned, the probability density under the assumption that the correction relative frequency for the W/L ratio in reverse and normal faults also approximates the single-side probability density function in normal distribution, as shown in Fig.9.

The uplift side of reverse faults in the Northeast Japan Inner Zone and the subsidence side of normal faults in the Kyushu region show large deviation of around $1\sigma=0.09$W/L, while the subsidence side of

reverse faults in the Northeast Japan Inner Zone also indicates the deviation in excess of 1σ=0.06W/L. Meanwhile, strike-slip faults in the Chubu and Chugoku regions as well as the uplift side of normal faults in the Kyushu region have a relatively small deviation of 1σ=0.03～0.04W/L.

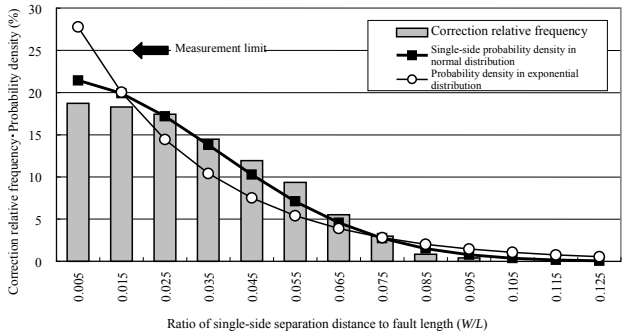

Fig.8 Comparison of the correction relative frequency and probability density function of the W/L ratio in strike-slip faults

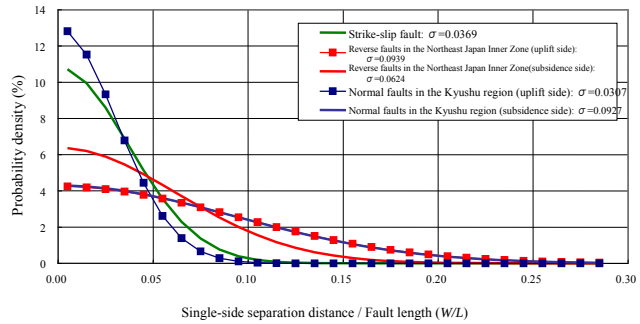

Fig.9 Single-side probability density function in normal distribution of *W/L* ratio according to fault type as well as uplift and subsidence sides

5. CONCLUSION

Making a probabilistic assumption on the range of influence from fault activities in the super long-term based on the findings of this study, enables the selection of suitable candidate sites for a disposal facility and reduces the risk of having to change candidate sites after reaching the stage of on-site investigation.

When combined with findings from separate studies on the range of influence from other natural events such as volcanic activities, the results of this study should provide one of judging criteria in selecting a site for building a special civil engineering structure that requires the maintenance of its functionality in the super long-term. The results may also be applied to compiling probabilistic data to be used in future studies concerning severe accidents.

ACKNOWLEDGEMENTS

I wish to express sincere gratitude to Professor Koichi Maekawa of Tokyo University for valuable advice he had provided during the course of this study, and to Dr. Tetsuya Fukuda of NEWJEC Inc. for providing insight into specific calculation approaches.

REFERENCES

1) Nuclear Waste Management Organization of Japan (2004): Evaluating Site Suitability for a HLW Repository (Scientific Background and Practical Application of NUMO's Siting Factors).

2) Matuda, T., Okada, S., Watanabe, T. (2004): Development of active strike-slip faults in Chugoku and Chubu districts –the comparison of cumulative slip, length of faults and width of crushed zones, Active Fault Research, 24, pp.1-12.

3) Kakimi, T., et al. (2003): A Seismotectonic Province Map in and around the Japanese Islands, Earthquake No.2, 55, pp.389-406.

4) Ranalli, G. (1977): Correction between length and offset in strike-slip faults, Tectonophysics, 37, pp.T1-T7.

5) Cartwright, J. A., Trudgill, B. D., Mansfield C. S. (1995): Fault growth by segment linkage: an explanation for scatter in maximum displacement and trace length data from the Canyonlands Grabens of SE Utah, J. Struct. Geol., 17, pp.1326-1326.

6) Walsh, J. J., Nicol, A., Childs, C. (2002): An alternative model for the growth of faults, J. Struct. Geol., 24, pp.1669-1675.

7) Cowie, P. A., Scholz, C. H. (1992): Physical explanation for the displacement-length relationship of faults using a post-yield fracture mechanics model. J. Struct. Geol., 14, pp.1133-1148.

8) The Headquarters for Earthquake Research Promotion (2010): Evaluations of active faults to date
http://www.jishin.go.jp/main/p_hyoka02_danso.htm

9) Active Fault and Earthquake Research Center, National Institute of Advanced Industrial Science and Technology (2010): Active fault database of Japan, Search for behavioral segments
http://riodb02.ibase.aist.go.jp/activefault/cgi-bin/search_map.cgi?search_no=j029&version_no=1&search_mode=0

10) Kano, K., Murata, A. (1998): Structural Geology VI.5 Extension and Shortening Tectonics of the Northeastern Japan Arc, Asakura Publidhing Co., Ltd., pp.256-262.

11) Kagohara, K., et al. (2006): Active Tectonics of the Senya Hills and Evolution of the Senya Active Fault, Eastern Margin of the Yokote Basin Fault Zone, Northeast Japan, Journal of geography, No.115,No.6,pp.691-714.

12) Kimura, M. (1990): Genesis and formation of the Okinawa Trough, The memoirs of the Geological Society of Japan, No.34,pp.77-88.

13) Itoh, Y., Takemura K., Kamata H. (1998): History of basin formation and tectonic evolution at the termination of a large transcurrent fault system: deformation mode of central Kyushu, Japan, Tectonophysics, 284, pp.135-150.

14) Ogata, S. (1976): Activity evaluation of fault in the basement terrain –characteristics of its fracture thickness and filled materials, Jour. Japan Soc. Eng. Geol., 17, pp.119-121.

15) Kanaori, Y. (2001): How Far does the Influence of Faulting Extend, Journal of the Japan Society of Engineering Geology, 41, pp.323-332.

16) Vermilye, J. M., Scholz, C. H. (1988): The process zone: A microstructural view of fault growth, J. Geophys. Res., 103, pp.12223-12237.

17) Yoshida, E., et al. (2009): Fracture Characterization along the Fault: A Case Study of 'Damaged Zone' Analysis on Atera Fault, Central Japan, Journal of the Japan Society of Engineering Geology, 50, pp.16-28.

18) Twiss, R.J., Moores, E.M. (1992): Structural Geology, 7, Strike-Slip Faults, W. H. Freeman and Company, New York, pp.113-127.

19) Ikeda, Y., et al. (2002): Atlas of Reverse Faults of the Quaternary Period, University of Tokyo Press, 254p.

20) Twiss, R.J., Moores, E.M. (1992): Structural Geology, 5,Normal Faults, W. H. Freeman and Company, New York, pp.74-95.